Supplementary information for

Living myofibroblast-silicon composites for probing electrical coupling in cardiac systems

Menahem Y. Rotenberg[a,1], Naomi Yamamoto[b], Erik Schaumann[b], Laura Matino[c,d], Francesca Santoro[c], Bozhi Tian[a,b,e,1]

[a]The James Franck Institute, the University of Chicago, Chicago, IL 60637, USA; [b]Department of Chemistry, the University of Chicago, Chicago, IL 60637, USA; [c]Tissue Electronics, Center for Advanced Biomaterials for Healthcare, Istituto Italiano di Tecnologia, 80125, Naples, Italy; [d]Department of Chemical Materials and Industrial Production Engineering, University of Naples Federico II, 80125, Naples, Italy; [e]The Institute for Biophysical Dynamics, Chicago, IL 60637, USA.

[1]To whom correspondence may be addressed. Email: hrotenberg@uchicago.edu or btian@uchicago.edu

www.pnas.org/cgi/doi/10.1073/pnas.1913651116

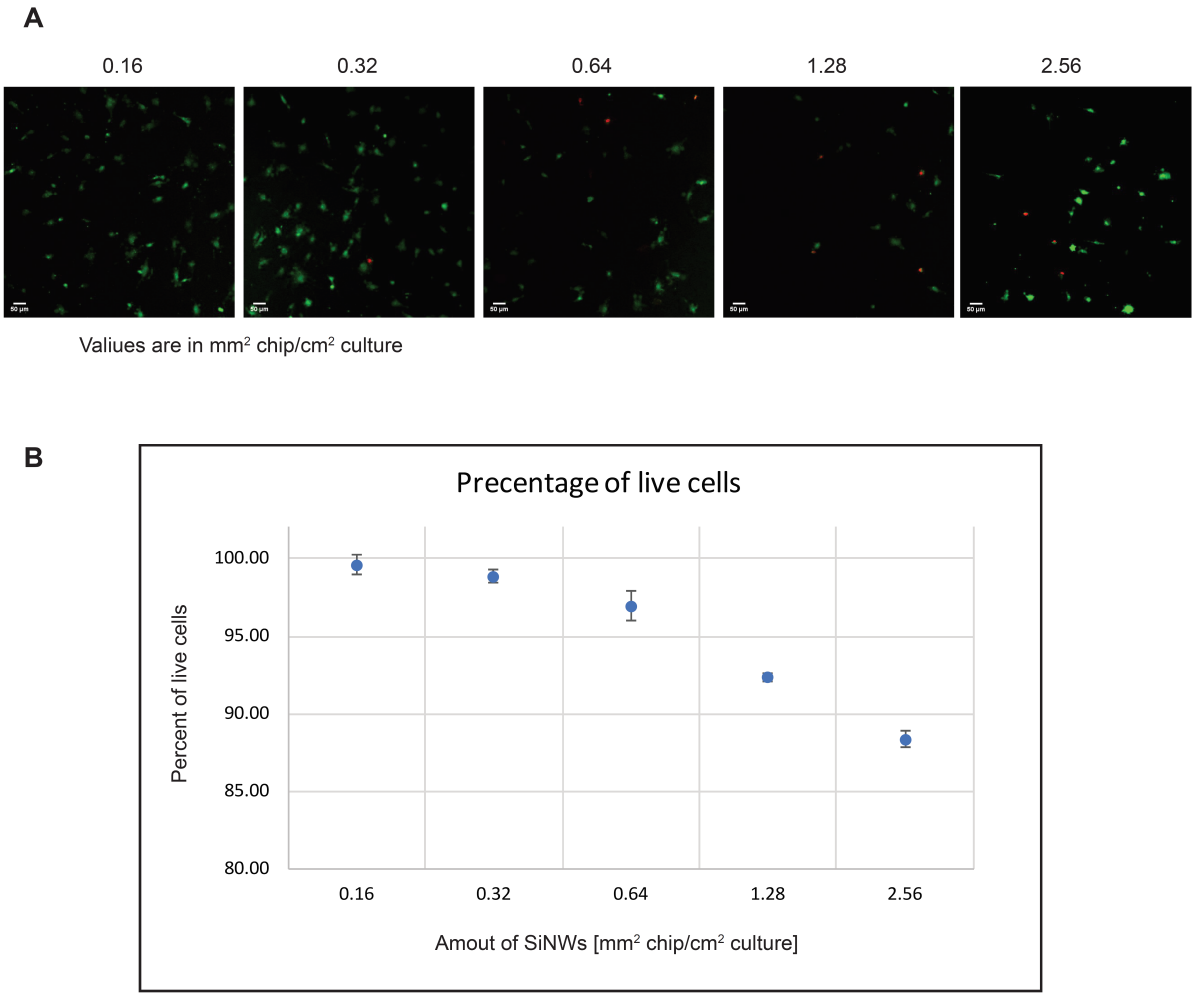

Supplemental Figure 1

Live/dead assay of MFs cultured with SiNWs. The effect of different SiNW concentrations on MFs' viability was investigated by counting live (green) and dead (red) cells after SiNW internalization. (A) Representative images of the cells with varying SiNW concentration. (B) Statistical quantification of the proportion of live cells in each image. In this study we used 9 mm^2 chip per 55 cm^2 culture dish area (see methods), corresponding to 0.16 mm^2 chip/cm^2 culture dish area. Higher SiNW concentration induce higher levels of cell death, likely due to overloading of SiNWs, which compromises the integrity of the plasma membrane.

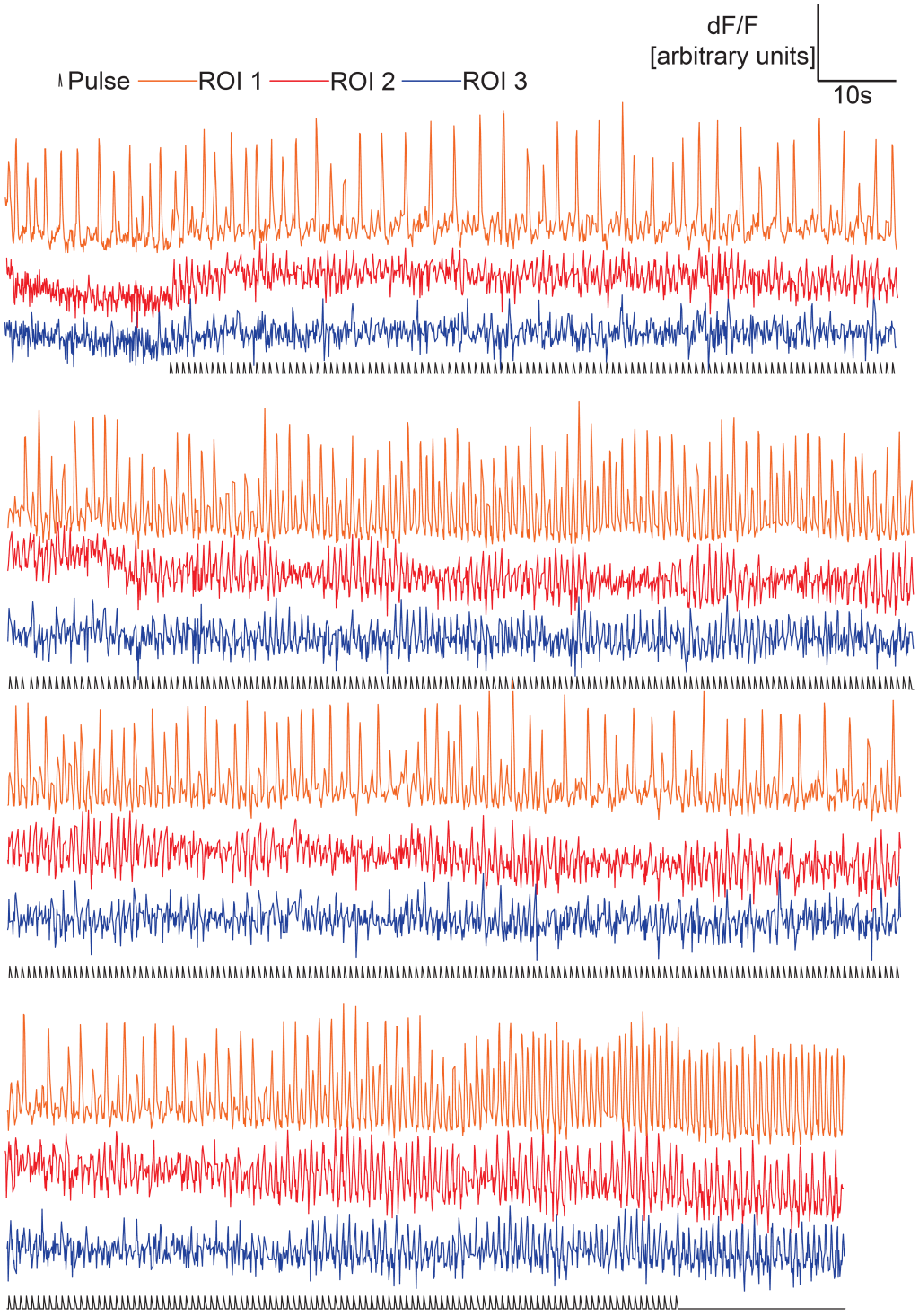

Supplemental Figure 2

Full presentation of the dF/F time profile of the 3 ROIs shown in **Figures 1 E-F**. The different responses to optical stimulation of the hybrid is illustrated for ~450s.

Example A:

Immediate response (7mW)

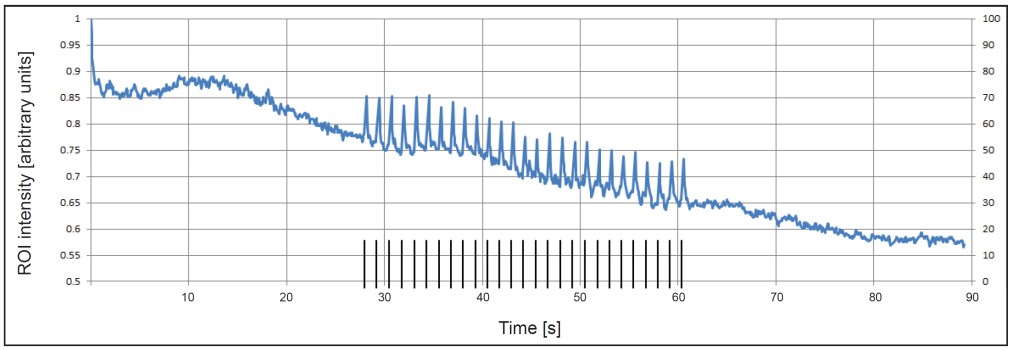

Example B:

Immediate response with damage to cells (7mW)

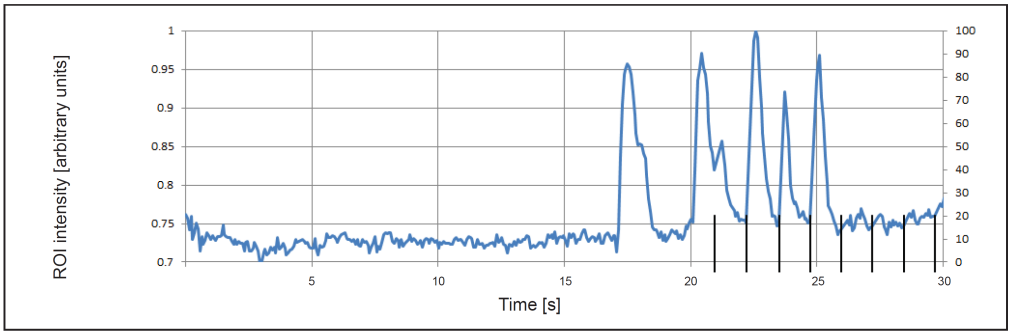

Example C:

Immediate response with damage to cells (7mW)

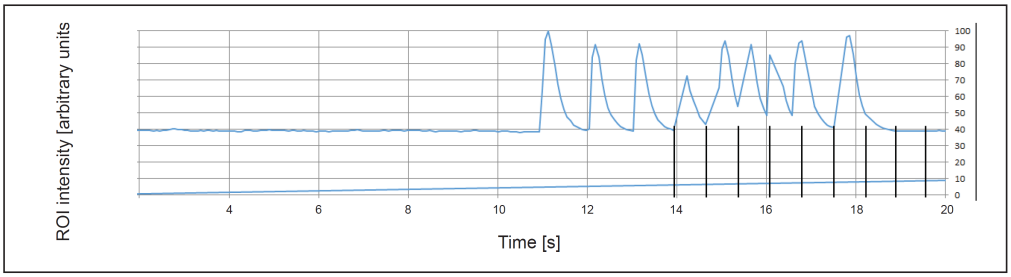

Supplemental Figure 3

To demonstrate that SiNWs have different responses to optical stimulation, we show the effect of stimulating hybrids with high (7 mW) laser power. Upon stimulation, the response of CMs to the stimulated hybrid was immediate. The CMs' electrical activity immediately synchronized to the laser pulses. However, this high-power laser stimulation produced excess energy that may have harmed the stimulated hybrid. Consequently, in two out of three cases presented here (examples B and C), the immediate response of the CMs did not persist over time. Thus, we decided to use the lowest power necessary to yield effects.

Example A:

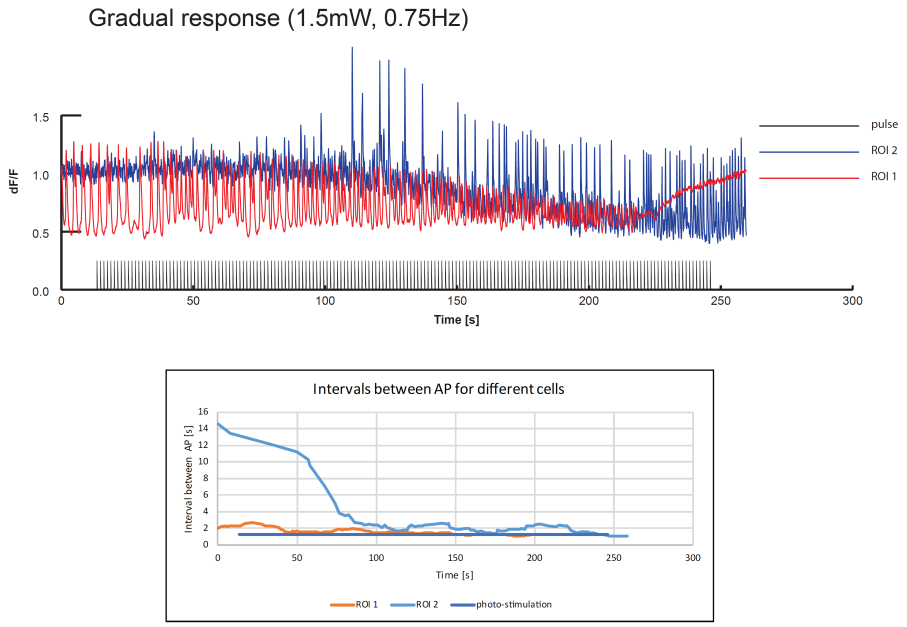

Example B:

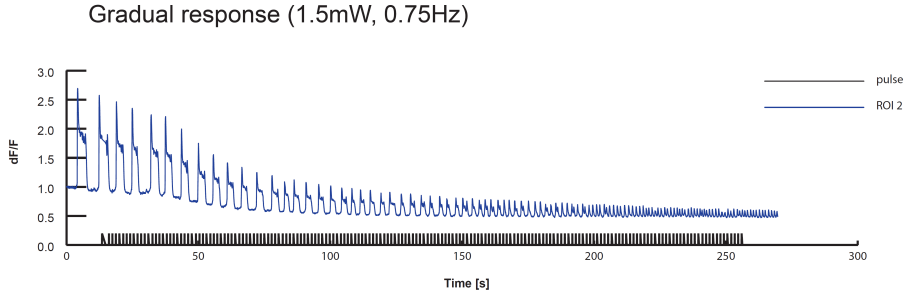

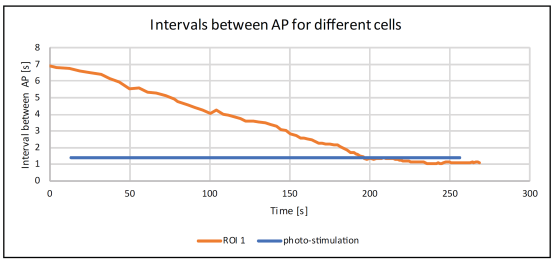

Supplemental Figure 4

To demonstrate that SiNWs have varying responses to optical stimulation, we show the effect of stimulating hybrids with low (1.5 mW) laser power. Upon stimulation, the response of the CMs to the stimulated hybrid was gradual, as in **Fig. 1E-G**. The CMs' electrical activity did not show any immediate change upon optical stimulation. However, continued stimulation at low power gradually increased neighboring CMs' activation rate until they were synchronized to the stimulation rate.

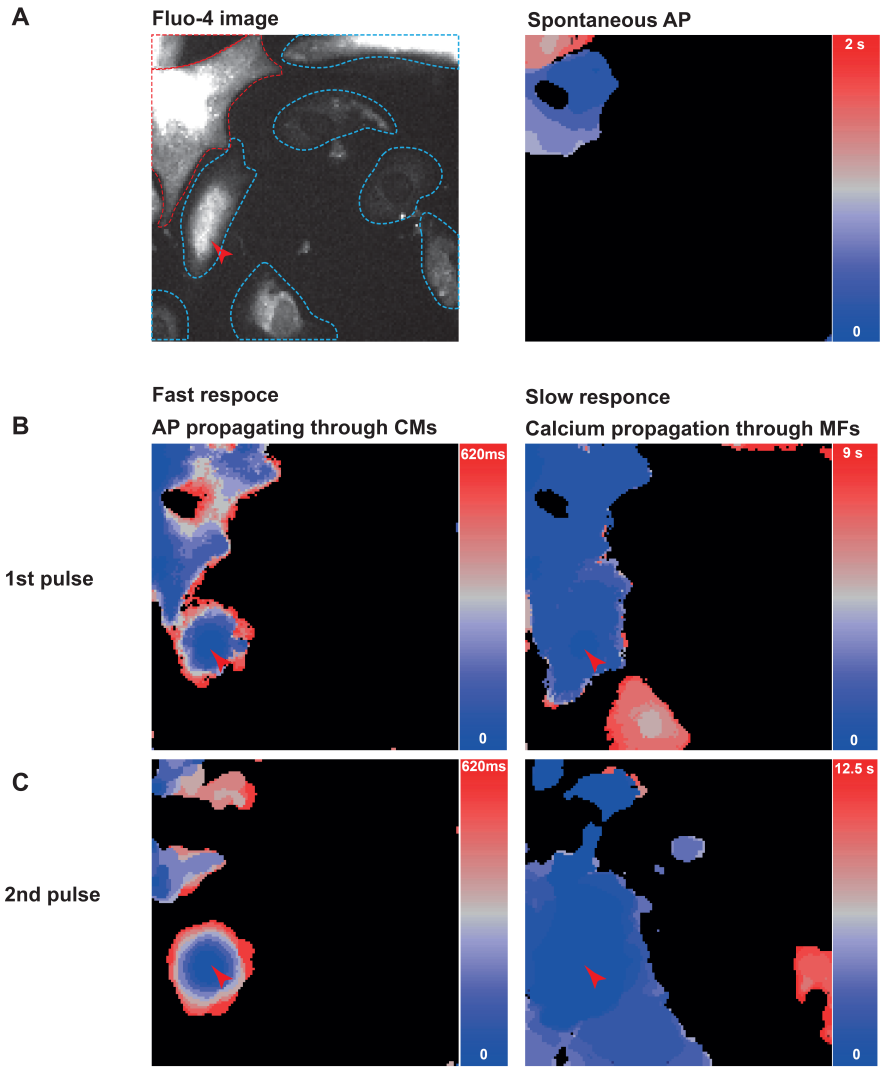

Supplemental Figure 5

Another illustration of the fast-slow response to optical stimulation of the hybrids. (A) A representative image (left) of the Fluo-4 loaded MFs (blue dashed lines) and CMs (red dashed lines). A spontaneous AP propagation is mapped, showing a relatively slow propagation rate between two adjacent CMs, while the MFs were inactive. (B) Upon optical stimulation, the MFs responded with a calcium flux that immediately propagated to the adjacent CMs (left). When examining the result at a longer time scale (right), it is seen that another wave of calcium flux slowly propagates through the MFs. (C) We repeated this with another laser pulse applied on the same SiNW, and the response was similar, suggesting that the stimulated hybrid is intact. Although the fast response of the stimulation was the same (the missing part of the CMs is due to oversaturation, precluding the use of dF/F measurements), the slow response wave propagated differently, with a faster response in the adjacent MF. The slow response wave also propagated further. This may suggest that the preceding depolarized state of the stimulated hybrid, which did not fully resume its baseline resting membrane potential, amplified the effect of the consecutive laser pulse and increased its effect.

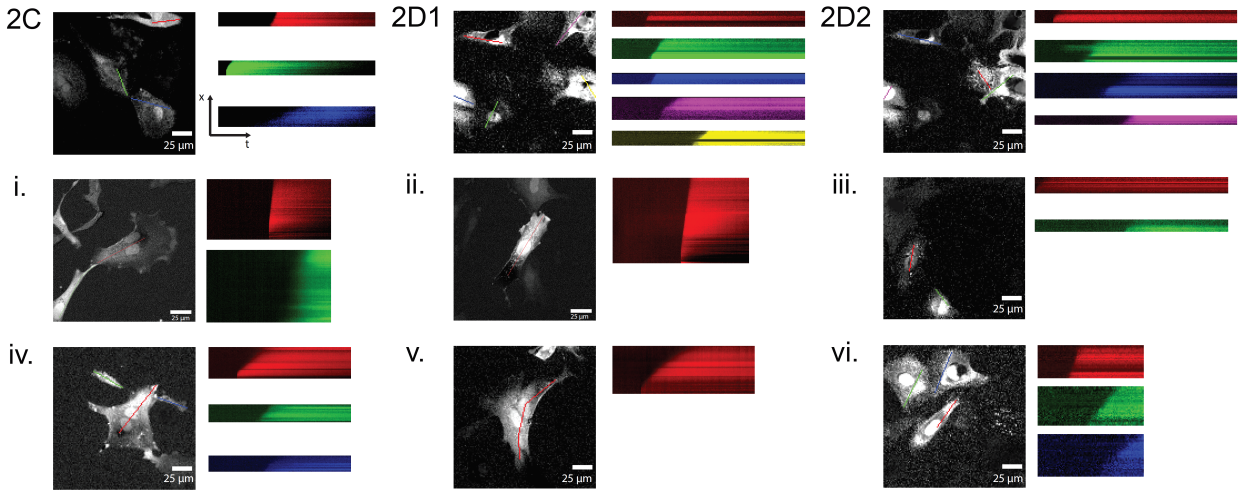

Supplemental Figure 6

Thresholded kymographs along the axis of calcium propagation after optical stimulation of the MF-SiNW hybrid. Tiles 2C, 2D1, and 2D2 correspond to the heatmaps shown in Fig. 2 C and Fig. 2D (left and right) in the main text, respectively. Tiles i-vi indicate measurements taken from samples that do not appear in the main text.

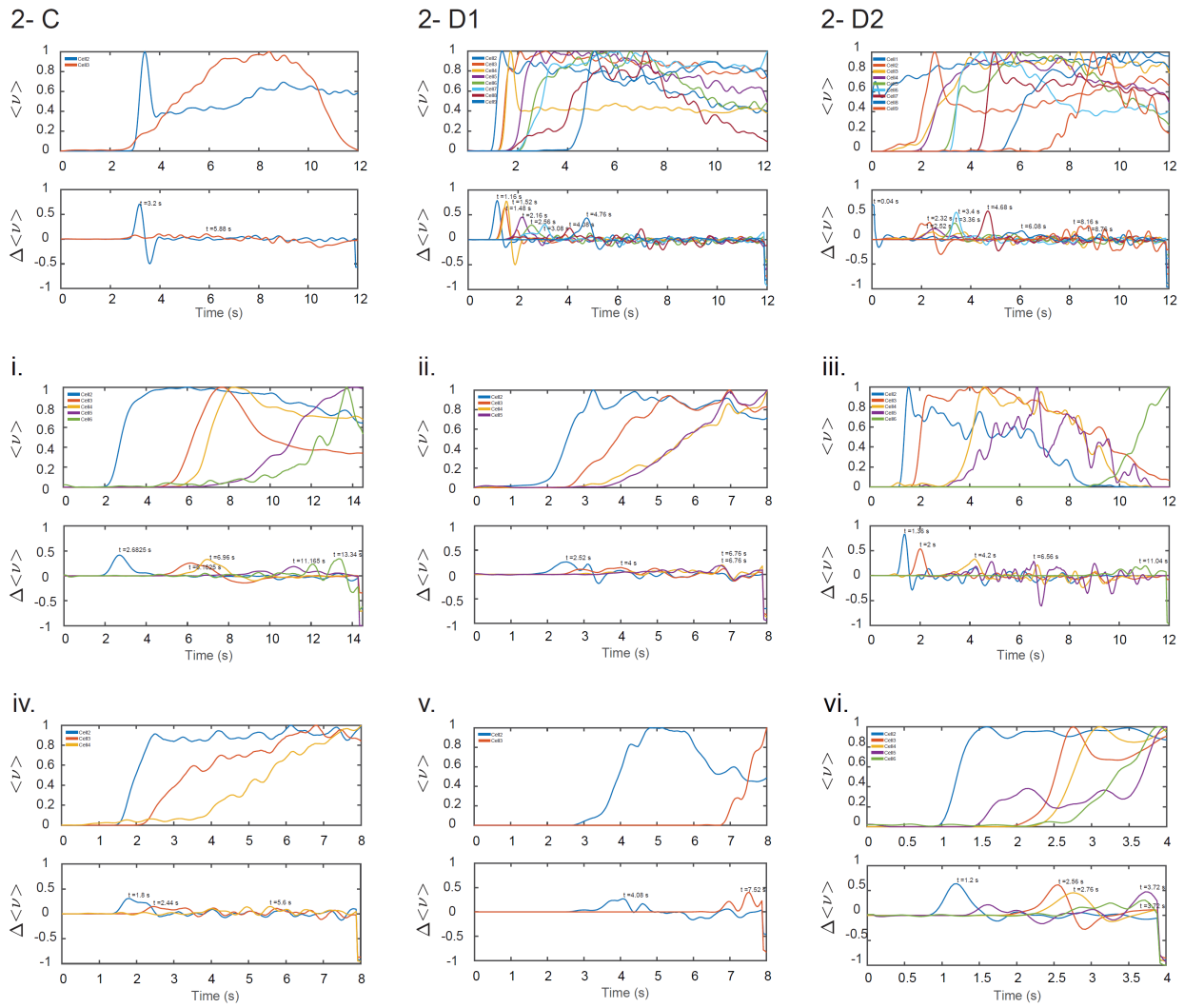

Supplemental Figure 7

Plots of <v>, the average optical flow, within individual cells as computed via the Lucas-Kanade algorithm (See **Methods, Optical Mapping**). Tiles 2-C, 2-D1, and 2-D2 correspond to the heatmaps shown in Fig. 2C and Fig. 2D (left and right) in the main text, respectively. Tiles i-vi indicate measurements taken from samples that do not appear in the main text. For ease of visualization, the <v> signal (top panel in each pair) is normalized to the highest value for each cell. The activation time of a cell is identified as the point where the differential Δ<v> (bottom panel in each pair) of the mean optical flow signal reaches its peak. Typically, the first cells to be stimulated also experienced a more rapid increase in <v>, such that the peak in Δ<v> decreases in value for cells with later activation times.

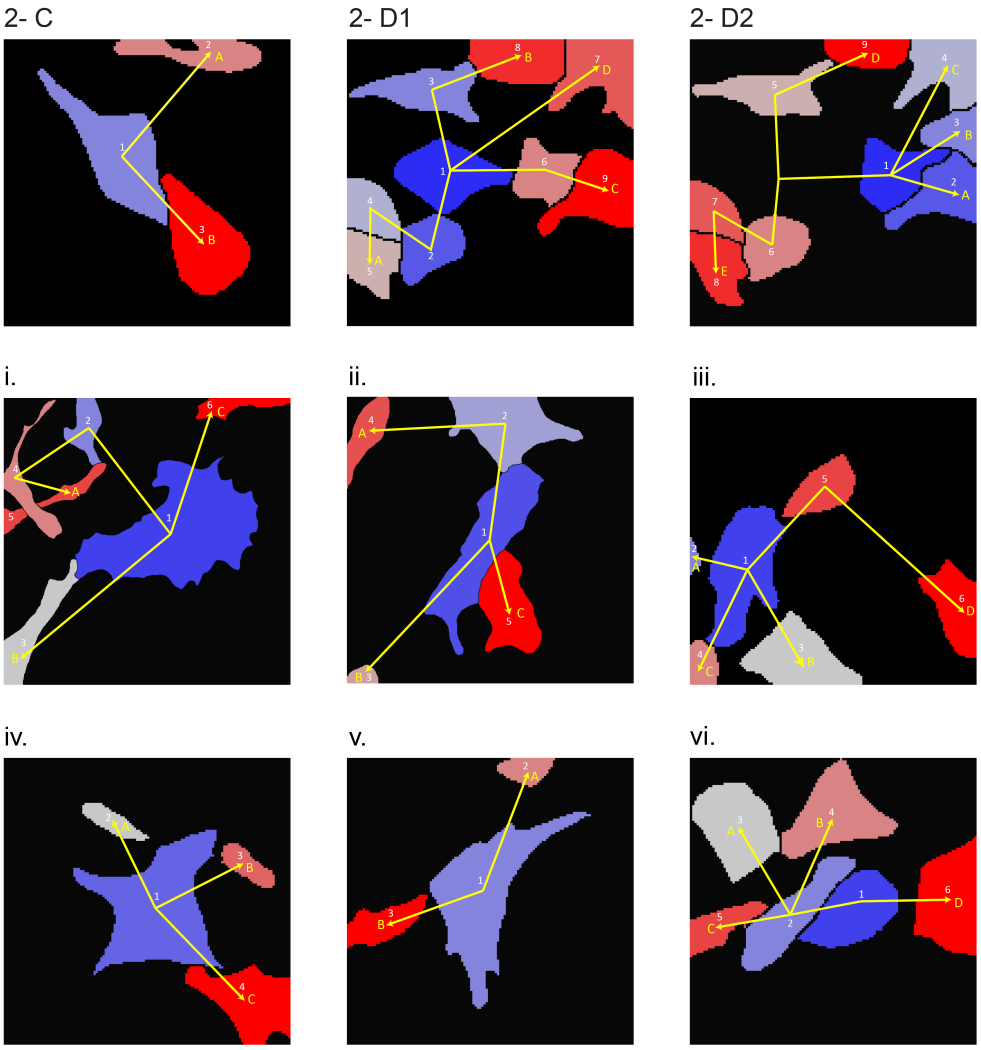

Supplemental Figure 8

Cell activation order. Based on **Supplementary Fig. S7** the order in which different cells were considered activated (the time to reach the maximum mean flow) the propagation directionality was determined. Tiles 2C, 2D1, and 2D2 correspond to the heatmaps shown in Fig. 2 C and Fig. 2D (left and right) in the main text, respectively. Tiles i-vi indicate measurements taken from samples that do not appear in the main text. For simplicity, the arrows are connecting cells at their centers of mass. The time of activation, relative to the arrows' length were then used to determine the intercellular velocity of the calcium propagation.

The schematics indicating the paths used to calculate the speed of intercellular calcium propagation. Each path (yellow arrows, labeled by alphabetical characters) originates at the stimulated cell and proceeds to neighboring cells (labeled by numerals) sequentially based on the time of activation, which is given in **Supplementary Fig. S7**. The intercellular distance is calculated as the distance between centers of mass for each respective cell. The speed of calcium propagation, then, was approximated by dividing this intercellular distance by the difference in activation times.

Example A:

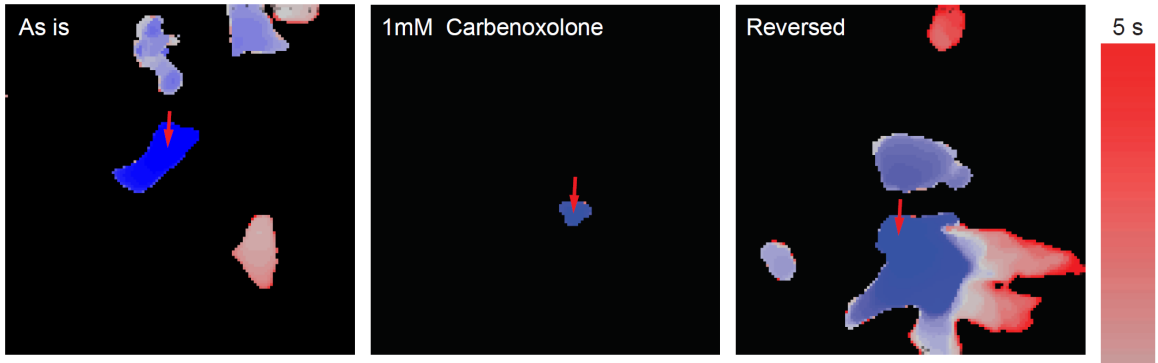

Example B:

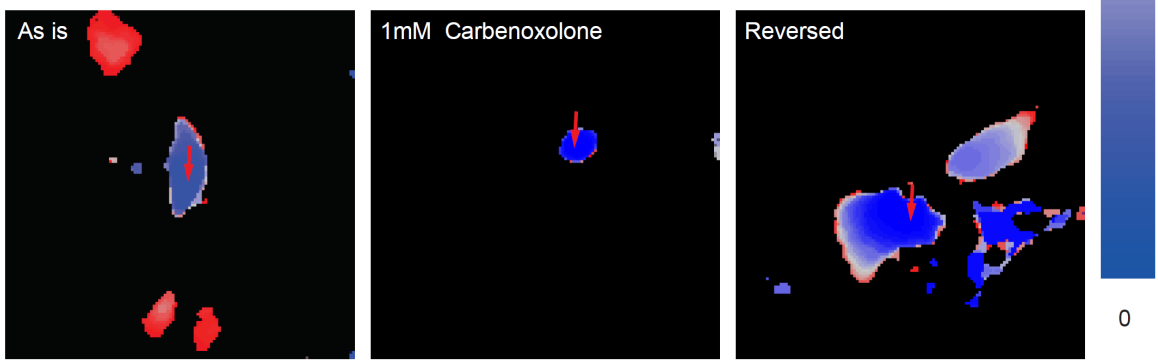

Supplemental Figure 9

The role of connexin 43 in mediating intercellular electrical coupling. Presented are two representative examples of the effect of carbenoxolone (connexin 43 blocker) on intercellular calcium propagation. Before adding carbenoxolone (left), calcium propagated from the stimulated cell (red arrow) to neighboring cells. Blocking connexin 43 gap junction (middle) completely abolished calcium propagation upon photo-stimulation. We then reversed the effect by removing the blockage (using carbenoxolone free fresh media) and demonstrated that intercellular calcium propagation can be restored (right).

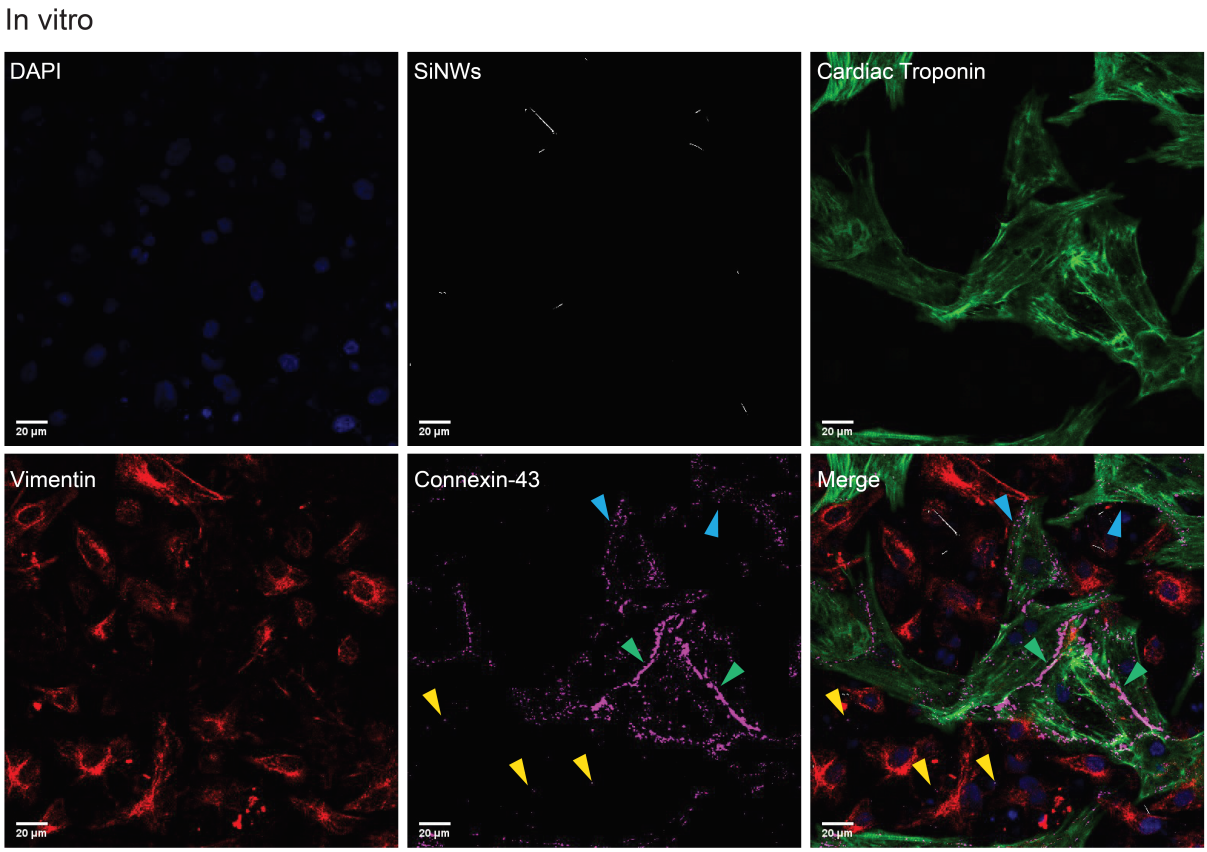

Supplemental Figure 10

Immunocytochemistry images of MFs (vimentin, red) and CMs (cardiac troponin, green) co-culture with nucleus staining (DAPI, blue), SiNWs (reflection, white) and connexin 43 staining (magenta). Dense connexin 43 plaques at the CM-CM interface are highlighted with green arrowheads. Lower amounts of connexin 43 are seen at the CM-MFs interface (blue arrowheads), while extremely low levels of connexin 43 are seen at the MFs-MFs interface (yellow arrowheads).

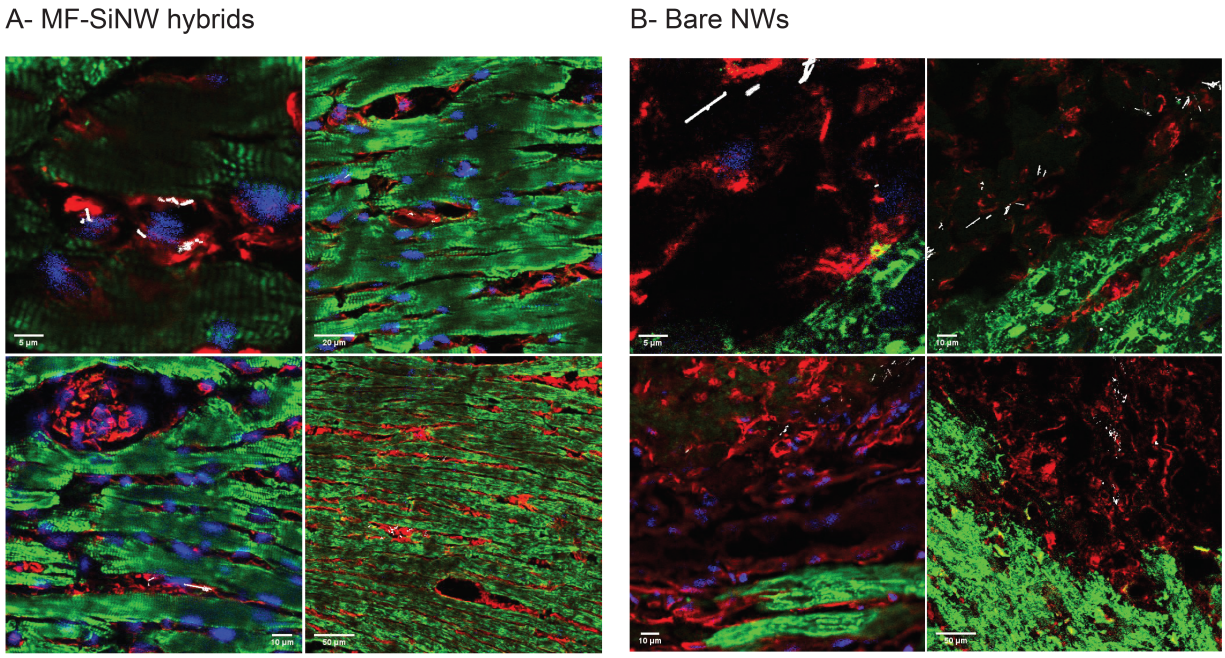

Supplemental Figure 11

Further examples of IHC stained cryo-sections, stained for cardiac markers: cardiac troponin (CMs, green), vimentin (MFs, red), DAPI (nuclei, blue), and SiNWs (reflection, white). (A) MF-SiNWs hybrids seamlessly integrate in to the native tissue with no apparent fibrotic encapsulation. (B) Injection of bare SiNWs results in thick fibrotic tissue encapsulating the NWs.

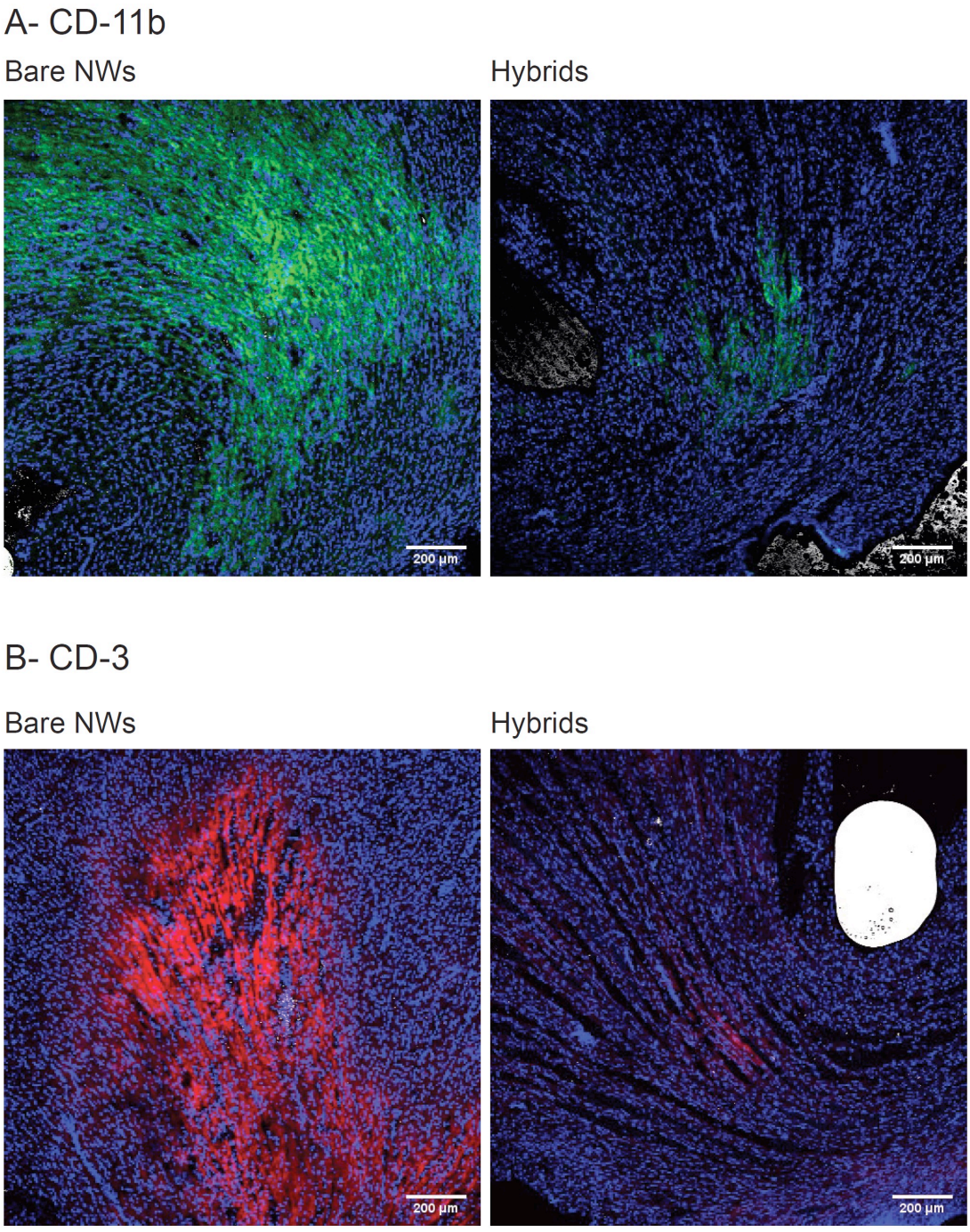

Supplemental Figure 12

IHC stained cryo-sections for immune response markers CD11b (A, green) or CD3 (B, red). Both also show DAPI (nuclei, blue) and SiNWs (reflection, white). Enhanced levels of immune markers in the vicinity of SiNWs are evident in the bare SiNWs group.

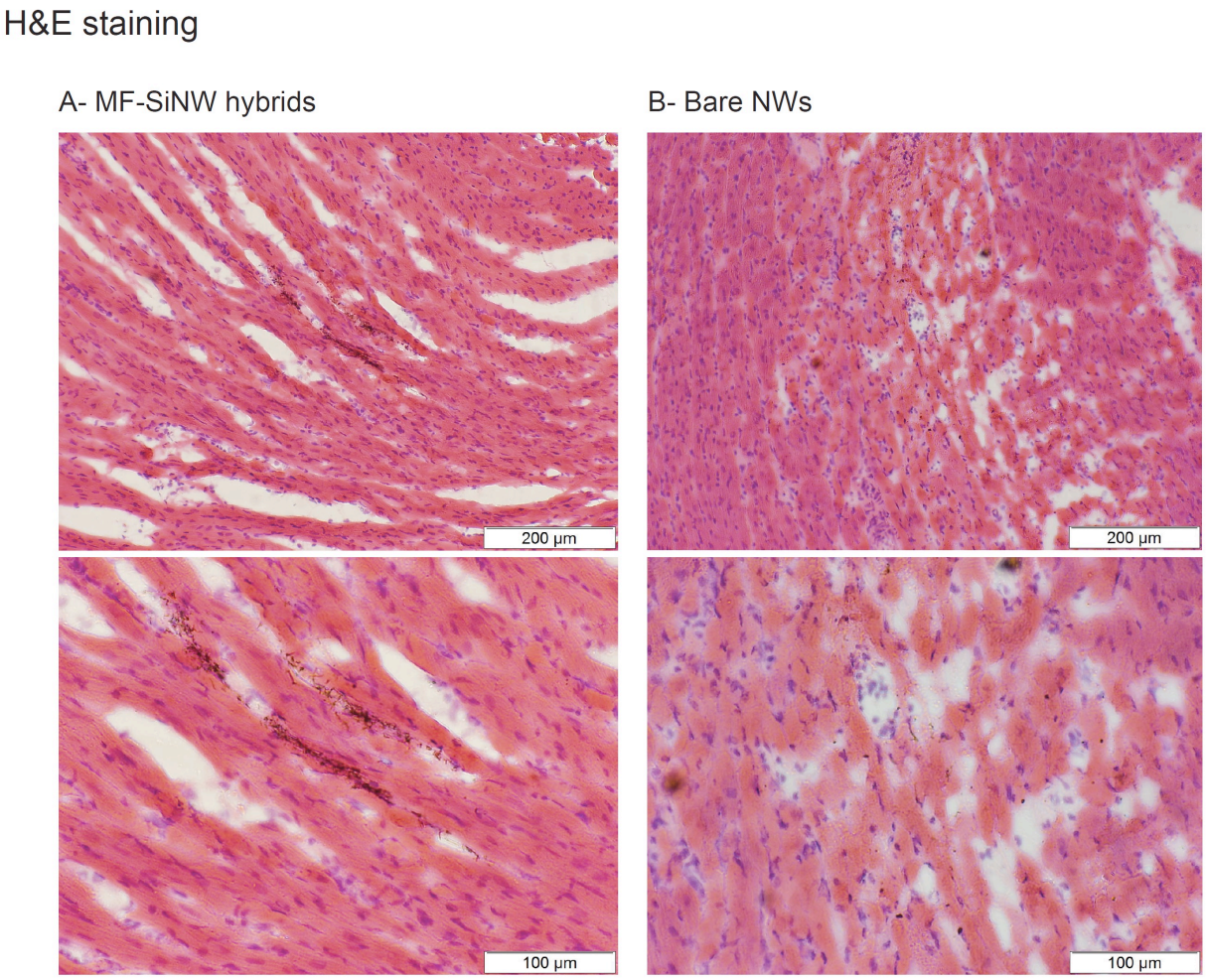

Supplemental Figure 13

Hematoxylin and eosin staining show: (A) striated cells adjacent to MF-SiNW hybrids and (B) deteriorated tissue around the bare SiNWs.

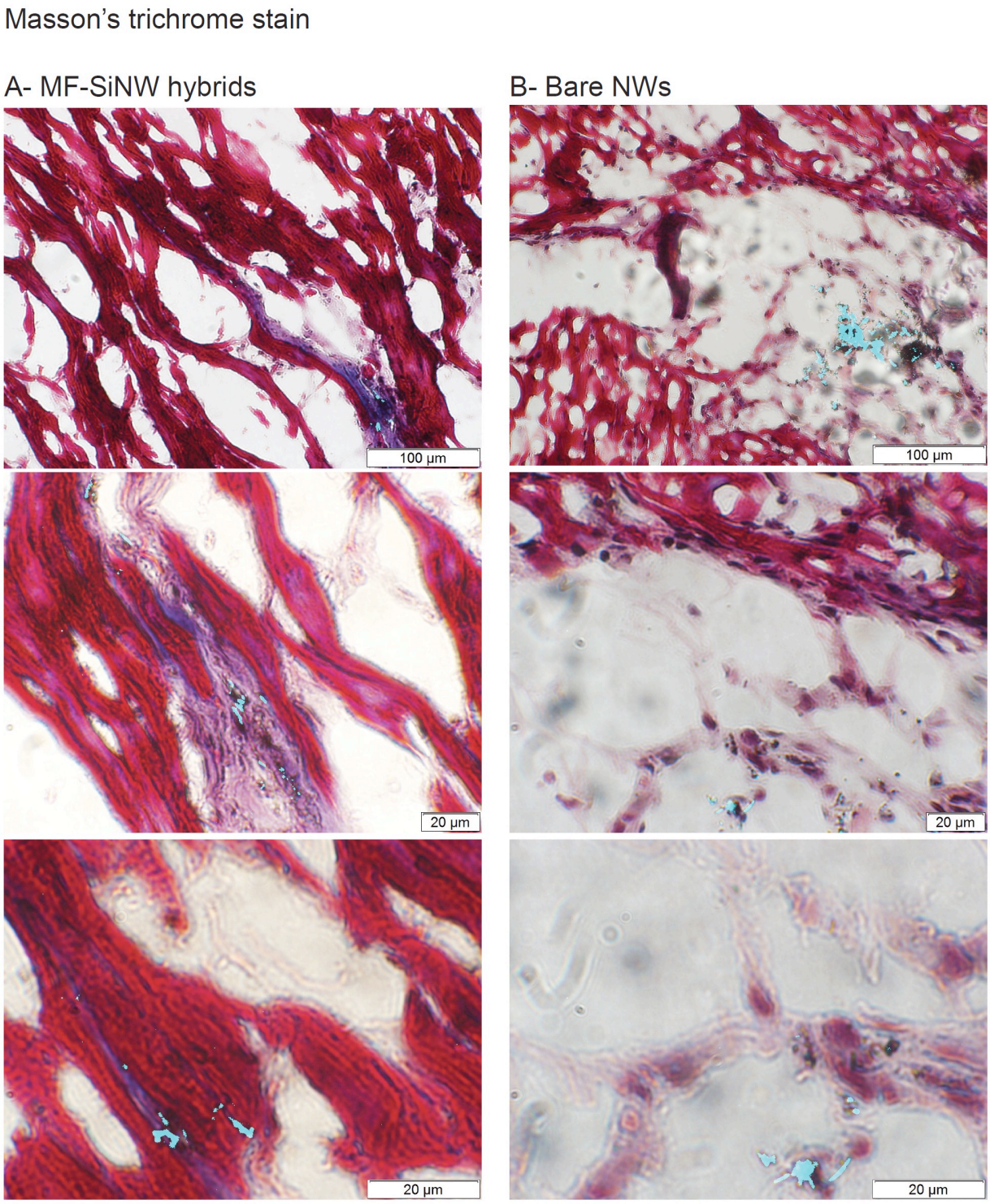

Supplemental Figure 14

Masson's trichrome stain shows cardiac muscle fibers in dark red. (A) SiNWs-MFs hybrids are seamlessly integrated with the muscle tissue and spread between the muscle fibers, while (B) clearly damaged, non-muscle tissue is observed around bare SiNWs.

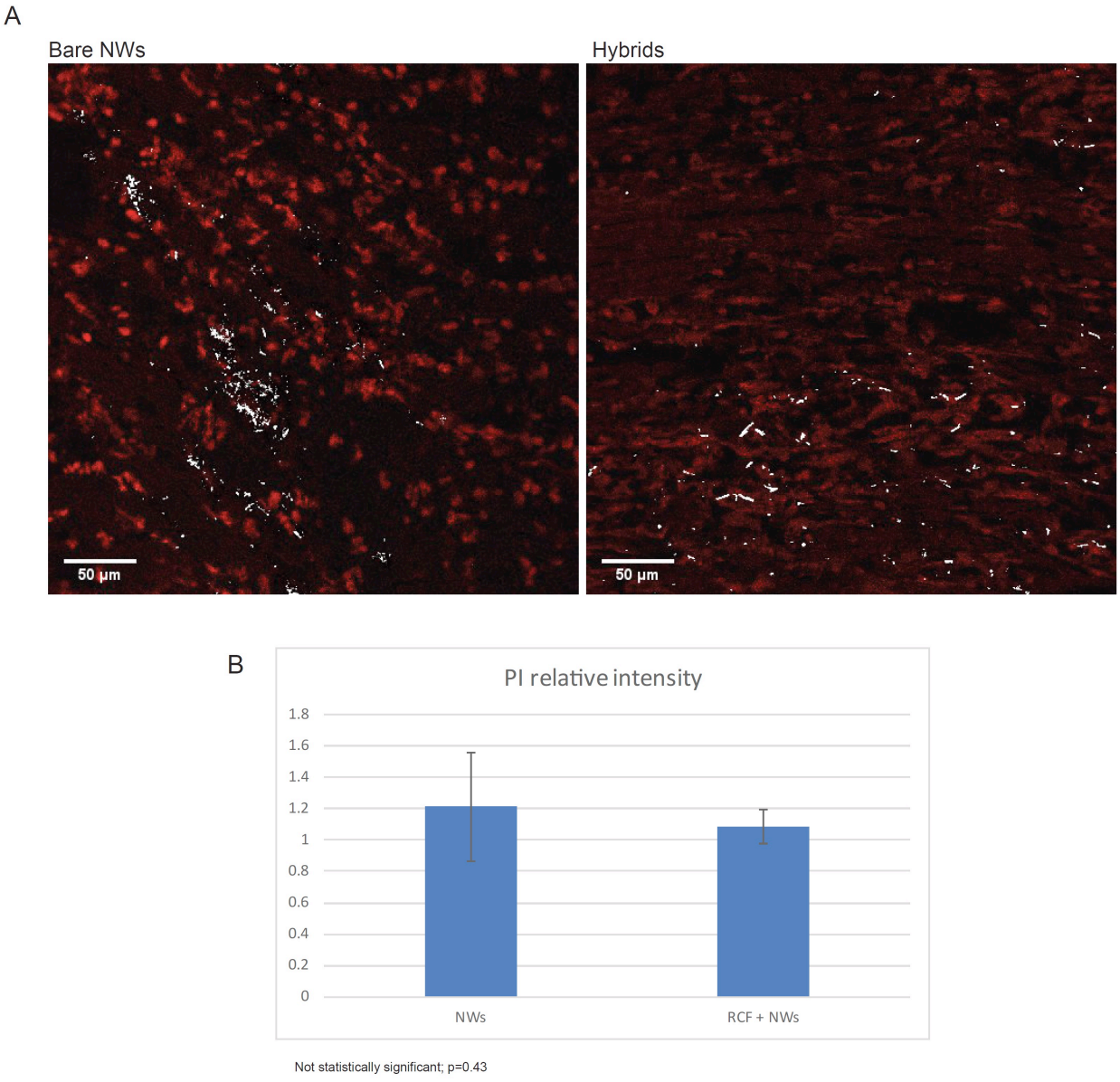

Supplemental Figure 15

After hybrids and bare SiNWs integrated with the tissue, the hearts were removed and perfused with propidium iodide. Then, the hearts were frozen in OCT and cut to 20µm cryo-sections. The areas surrounding the hybrids and bare SiNWs were (A) imaged for dead cells and (B) compared in terms of propidium iodide staining. No significant difference between the two samples was obtained (p=0.43).

In vivo

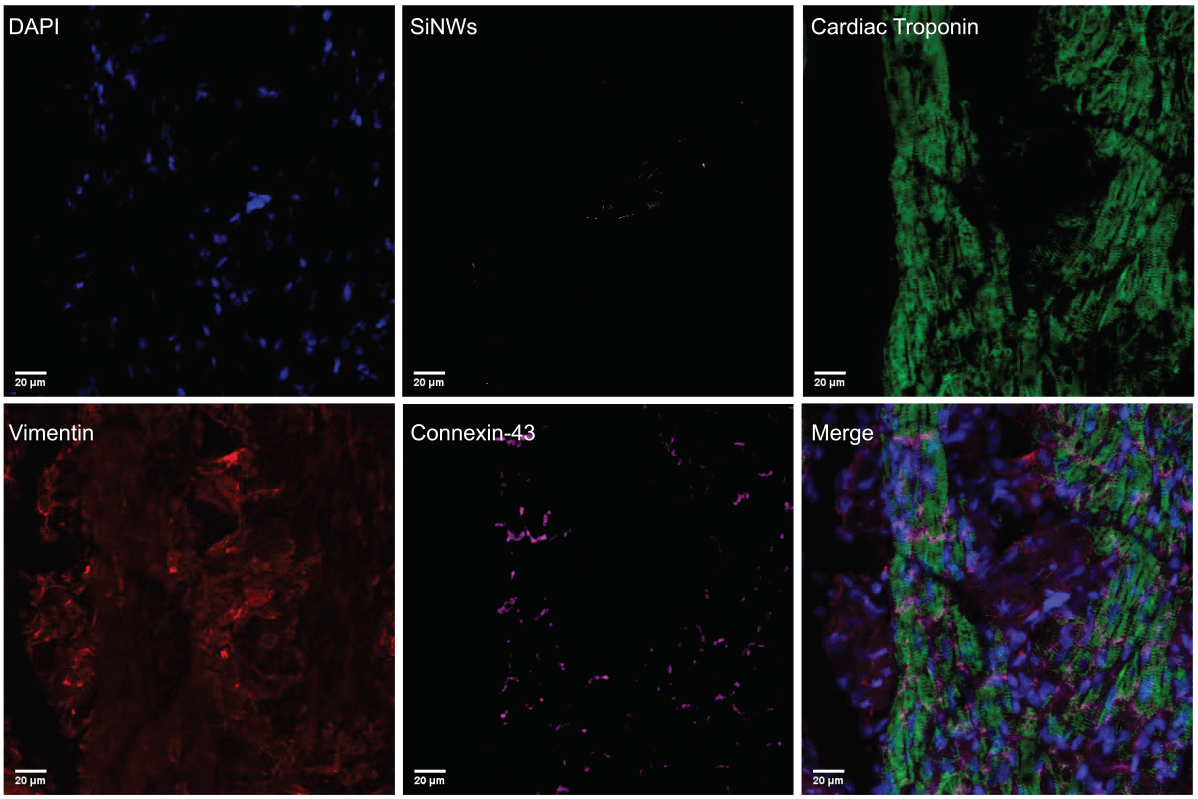

Supplemental Figure 16

IHC images of MFs-SiNWs hybrids transplanted in the native heart. Staining for MFs (vimentin, red), CMs (cardiac troponin, green), gap junction (connexin 43, magneta), nucleus staining (DAPI, blue) and SiNWs (reflection, white) show dense connexin 43 at the CM-CM interface. However, MFs regions appear to lack any connexin 43 based gap junction, supporting the hypothesis of low or no coupling of CMs-MFs in vivo.

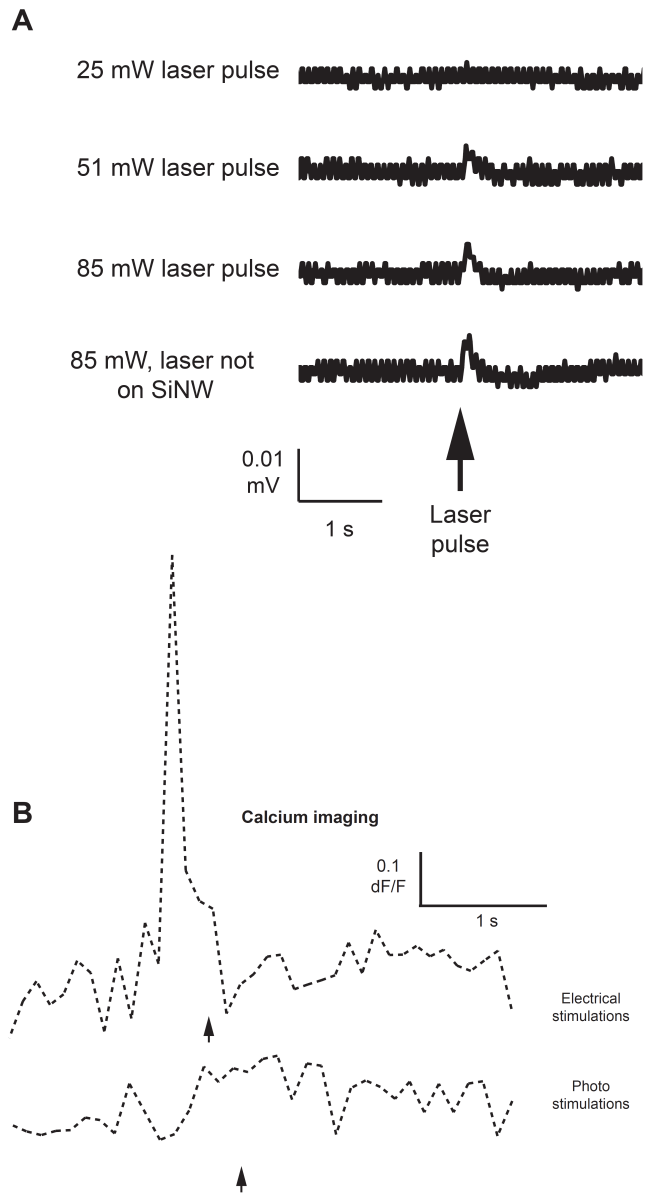

Supplemental Figure 17

Heart slices show negligible responses to optical stimulation. (A) Heart slices were stimulated with the STED laser while performing simultaneous ECG recording. The effect of different levels of laser stimulation power is shown. The fact that the artifact increases with laser power supports the notion that it is not related to an AP, as AP maintain a binary yes/no response independent of laser power. In addition, the amplitude of the artifact is much lower than the signal produced by a spontaneous slice contraction (see **Fig 4D**). Moreover, the artifact also appeared when the laser pulse was applied away from a SiNW. (B) Calcium imaging of a heart slice after MFs-SiNWs hybrids were integrated for 9 days. Top: Tissue is healthy and responsive to standard electrical stimulation (positive control). Bottom: Optical stimulation has negligible effect on the surrounding tissue.

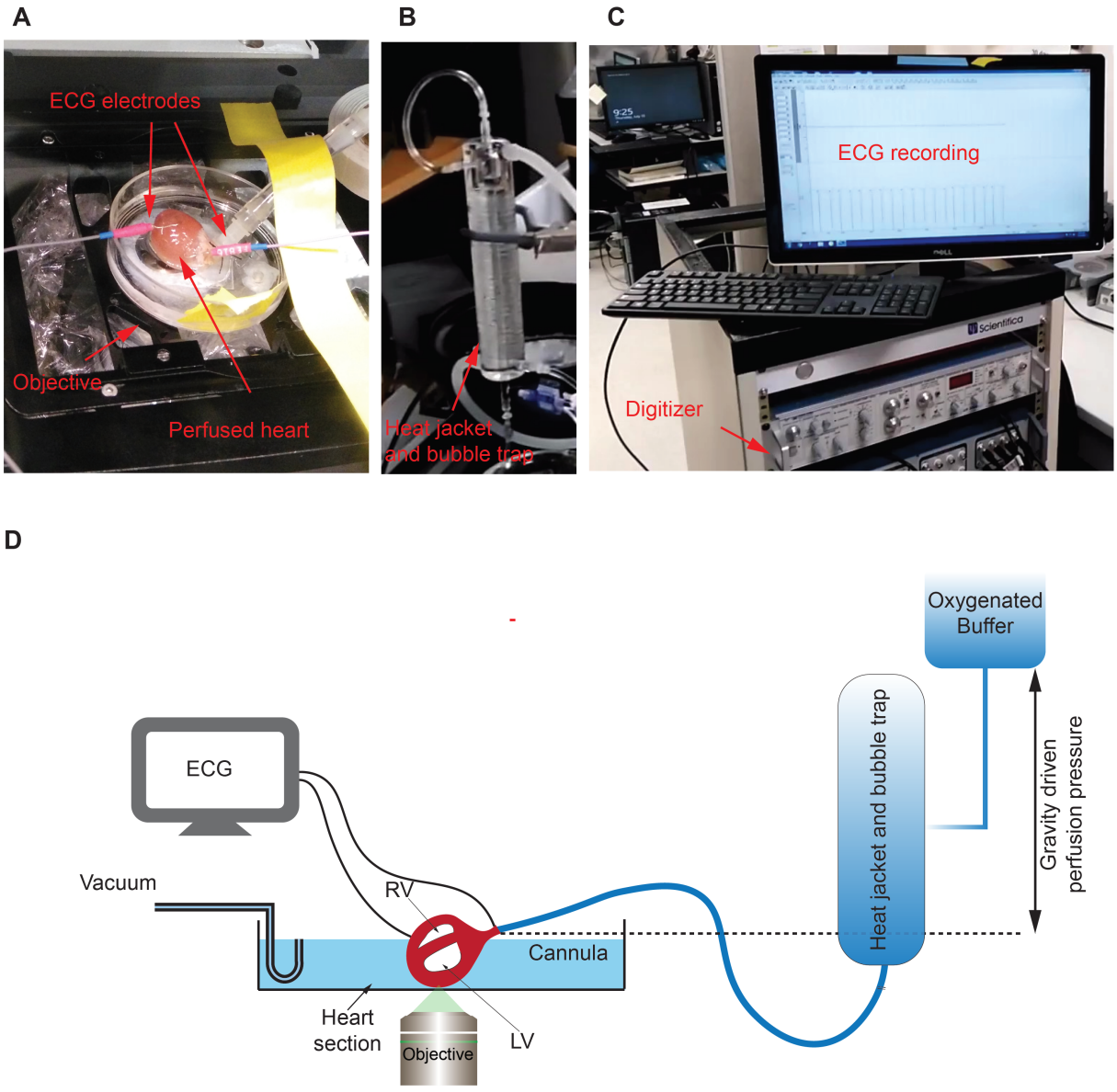

Supplemental Figure 18

The setup for the whole heart model in the confocal microscope. (A) The objective turret was covered with nylon to prevent fluids from entering the microscope setup. The heart was placed in a dish with glass bottom and a pre-mounted U-shaped vacuum tube to remove excess perfusion fluids. Two electrodes were used to monitor the ECG throughout the experiment. (B) A water-jacketed bubble trap was used to warm the perfusion buffer. (C) A digitizer was connected to the computer to monitor the ECG while another PC is controlling the microscope. (D) Schematic diagram of the setting used for the Langendorff apparatus.

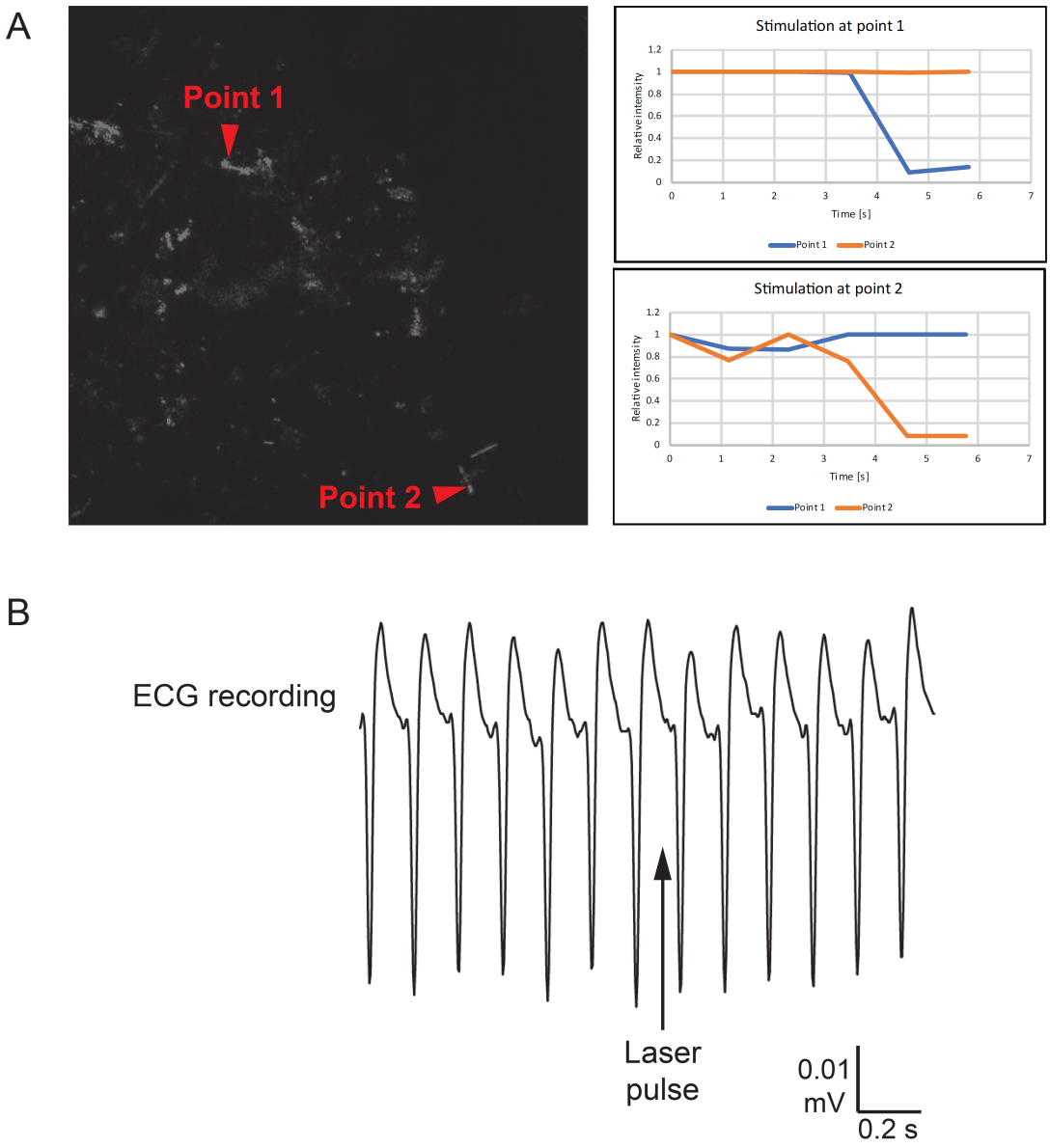

Supplemental Figure 19

High power photo stimulation did not elicit an AP in a whole isolated heart apparatus. (A) A representative reflected light image of the SiNWs inside the heart (left). Optical stimulation occurred at each point, and measures of reflected light at each region is plotted (right). Decrease in reflection at a particular point indicates that the SiNW moved out of the region of interest due to the thermal effect of photostimulation. (B) A representative ECG recording of the experiment showing stimulation with 85 mW power did not alter pacing, even though the SiNW clearly moved.

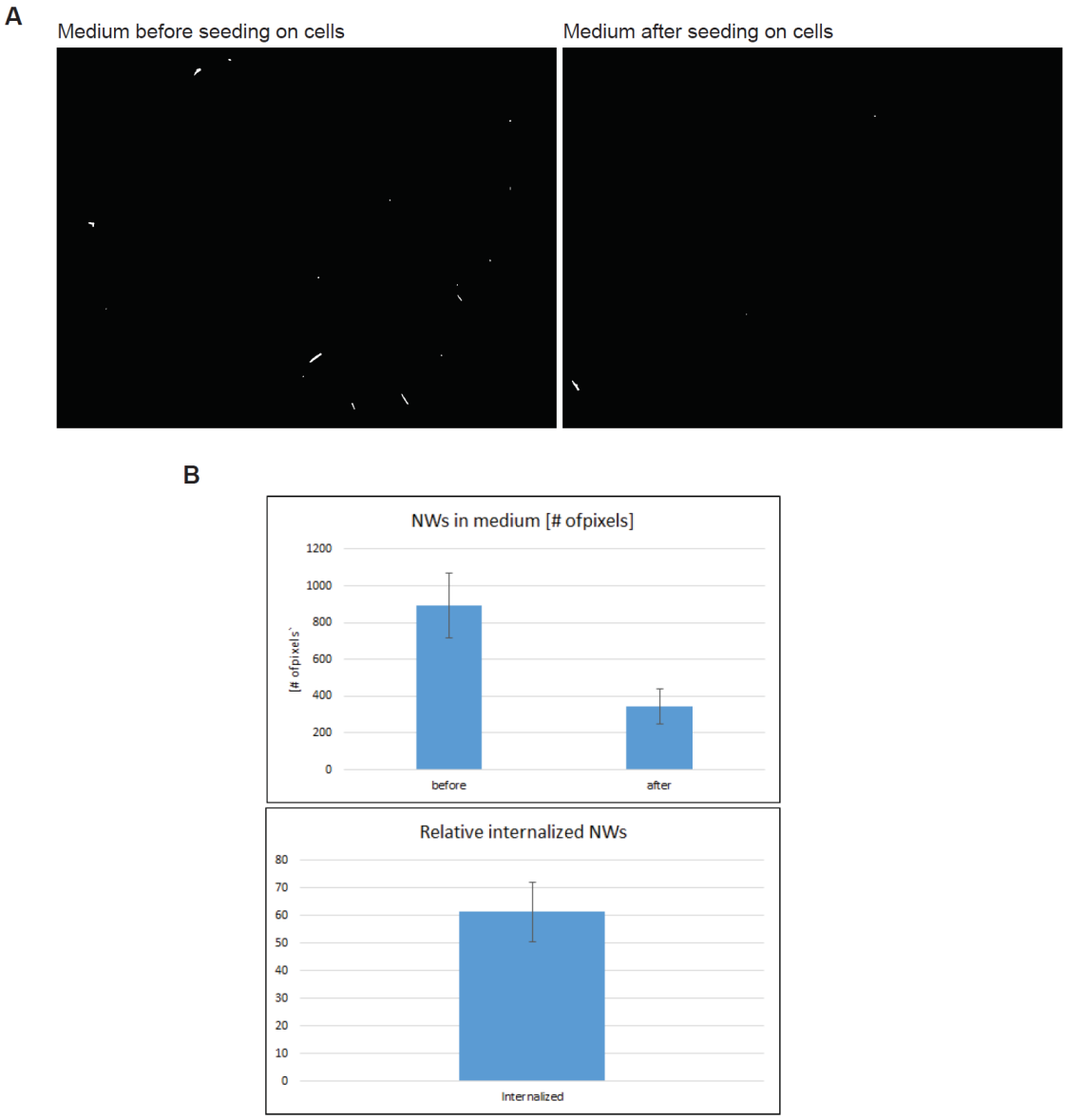

Supplemental Figure 20

Calculating an approximation of the amount of internalized SiNWs. (A) To approximate the amount of SiNWs that were internalized by the MFs, we imaged the suspended SiNWs in the media before and after internalization (A) and calculated the number of pixels that were positive for SiNWs (B). This value correlated to the amount of SiNWs in the suspension (all frames were given the same threshold). In this case we did not care for the absolute number of SiNWs, but for the area they have occupied. Then we derived from the proportion of SiNWs that were "missing" in the suspension, thus internalized in the MFs (bottom). According to this ratio, we used half the amount of SiNWs that were internalized as the control of bare SiNWs injected in vivo.

Supplemental Movie S1

The effect of the MF-SiNW hybrid pacing is presented by the Fluo-4 raw video (left) and the processed dF/F (middle) and binary (right) videos. The CMs rate is illustrated before and after the pacing for comparison.

Supplemental Movie S2

The two different propagations, MF-CM (fast) and MF-MF (slow), as shown in Figure 2 B-C, are represented by the Fluo-4 raw video (left) and the processed dF/F (middle) and binary (right) videos. The spontaneous activity of the CMs before the stimulation is shown, followed by the optically induced AP (immediately after the laser pulse), and then the slow MF-MF propagation.

Supplemental Movie S3

The slow MF-MF propagations described in Figure 2D are represented by the Fluo-4 raw video (left) and the processed dF/F (middle) and binary (right) videos. The different locations are shown by a red circle. Of note, these are the same cells in both stimulations, just different locations.

Supplemental Movie S4

The transplanted heart within the recipient rat's abdomen is viable and contractile 5 d after transplantation.

Supplemental Movie S5

A viable tissue slice contracting upon electrical stimulation.